International Journal of Pure and Applied Mathematics
Volume 117 No. 21 2017, 843-855
ISSN: 1311-8080 (printed version); ISSN: 1314-3395 (on-line version)
url: http://www.ijpam.eu
Special Issue

A Guided Image Fusion Approach for Spectral Compressed Sensing based Optimal Compression Plane Video Compression

[1]P. Kavitha and [2]Anna Saro Vijendran

[1]Department of Computer Science,

S.N.R. SONS College,

Coimbatore, Tamil Nadu, India.

kavithaphd2015@gmail.com

[2]Department of Computer Applications,

S.N.R. SONS College,

Coimbatore, Tamil Nadu, India.

saroviji@rediffmail.com

Abstract

The hybrid of Discrete Wavelength Transform (DWT) and Discrete Cosine Transform (DCT) (HDWT-DCT) was used to enhance the compression ratio with high-quality. This technique integrating optimal coding plane determination procedure to be used as a preprocessing step prior to any standard video coding method. Moreover, the Fast Continuous Linearised Augmented Lagrangian Method (FCLALM) was used to reconstruct the sparse coefficients from the combined measurement. However, the compressed image after eliminating some of spatial and spectral redundancy may need to be presented effectively through combing the image frames. Hence, the guided filtering method is introduced for image fusing that is used reduce memory size as well as to enhance the image quality after compressing the frames. Experimental outcomes show that our proposed technique is providing better results in terms of Maximum Difference (MD), Maximum Error (ME), Peak Signal to Noise Ratio (PSNR), Normalized Absolute Error (NAE) and Mean Square Error (MSE).

Key Words: Image Fusion, Guided Filter, Image Frames, Hybrid of Discrete Wavelength Transform (DWT) and Discrete Cosine Transform (DCT) (HDWT-DCT), Fast Continuous Linearised Augmented Lagrangian Method (FCLALM)

1. Introduction

Mainly applications in the areas of image processing and computational photography want smoothing approaches that might be protect edge well. This scheme usually decomposes an image to be filtered into detail and base layers. A detail layer was both noise and a base layer created through homogeneous regions with sharp edges. There are subsequent forms of edge-preserving image smoothing approaches. Filters using Global optimization (GO) is first form (He, K., et al 2013). A data and a regularization term based on the optimized presentation criterion. The data term calculates reliability of reconstructed image and that image to be filtered even as the regularization term produces the smoothness level of the reconstructed image. Despite the fact that the GO based totally on filters often yield excellent quality, they have excessive computational cost. Neighboring filters in bilateral filter (BF) is a second form (Li, Z., et al 2013), its adding in trilateral filter, gradient domain (Pham, C. C., et al 2012) and their accelerated models in addition to guided image filter (GIF). Generally simpler of the neighboring filters compared the global optimization based filters. But, the neighboring filters cannot generate halo artifacts and protect sharp edges.

In the previous work, the hybrid of DCT and DWT (HDCT-DWT) was proposed for enhance the compression ratio with good quality. This approach incorporating optimal coding plane determination process to be used as a preprocessing step prior to any standard video coding scheme. Moreover, the FCLALM was introduced to reconstruct the sparse coefficients from the jointed measurement. But, the DWT are used to reduce the sparse coefficients and the compressed image after eliminating some of spatial and spectral redundancy may require to be presented effectively via combing the image frames.

In this paper, we propose the guided filtering (GF) scheme for image fusing (IF). This technique is used to decrease memory size as well as to enhance the image quality after compressing the frames. IF is the manner of incorporating related information from more images into a single image. The ensuring image may be more informative than any other input images. Guided filter has less computation time which is independent of filtering size. In this approach, first the image will be changed into the two scale representation via applying the AF (average filtering) methods. In two scale representation, to change the image into the two representation like detail and base layer. Detail layer is defining the small scale variations and base layer is explaining the large scale variations. After change of each frame into the two scale representation, the GF based totally on weighted average scheme will be applied on the frames to fuse the detail and base layers.

The rest of the article is structured as follows: In Segment 2, explanation of images or videos compression schemes is given. In Segment 3, proposed schemes are described. In Segment 4, demonstrate the overall experimental

outcomes of the proposed techniques. In Segment 5, conclusion of the research work is given.

2. Related Work

Multi-View Video Coding (MVC) using efficient compression method for Integral Images (Shi, S., et al 2011) was introduced for sub-images (SI). The sub image becomes another form of 2D image changed from original integral image. Each and every sub image denotes the 3D scene from parallel viewing directions. Then consists of superior compression skills than source captured elemental images. Consequently, consider ordering the group of sub images because the design of multi-view video (MVV) after that encode the created MVV through MVC standard. An improved medical image compression method using region of interest (ROI) (Zuo, Z., et al 2015) becomes proposed to maximize compression. First, the image segmentation was used to divide the image into two parts: ROI regions and non-ROI regions. Lossless compression algorithm was applied to the marked area of ROI, and image restoration method and the wavelet-based lossy compression algorithm are utilized to the other area of the image. However, this approach produces excessive over-segmentation.

A hardware-friendly approximation to an presented fast dynamic range compression with local contrast preservation (FDRCLCP) algorithm (Li, S. A., & Tsai, C. Y. 2015) was proposed. In this approach, the computation of approximated FDRCLCP algorithm requires only fixed-point unsigned binary addition, multiplication, and bitshifting. In addition, the hardware implementation uses a line buffer instead of a frame buffer to process whole image data. Transforms based on 2D Markov Processes and Block-Based Spatial Prediction for Video and Image Compression (Kamisli, F. 2015) was proposed. The derived overall intra-frame coding technique was used to generalize the two techniques, provides produces less blocking effects and enhanced coding gains at low bitrates while increasing computational complexity. However, parameter estimation was computationally more expensive of this approach.

An efficient image compression–encryption method using hyper-chaotic system and 2D compressive sensing (Zhou, N., et al 2016) was proposed. The source image was calculated through the measurement matrices in two directions to achieve encryption and compression. At the same time, and then the out coming image were re-encrypted via the cycle shift operation (CSO) controlled via a hyper-chaotic system. CSO performed to modify the values of the pixels efficiently. Simpler image compression method using hybrid wavelet transforms (HWT) and vector quantization (VQ) (Kekre, H. B., et al 2016) was proposed. HWT was produced by Kronecker product of two different transforms. Image changed to transform domain via HWT and very few small frequency coefficients are kept to attain high-quality compression. VQ was applying on those coefficients to increase compression percentage considerably. However, encoding method was very expensive of this technique.

Low-Complexity Enhancement Layer Compression for Scalable Lossless Video Coding based on High Efficiency Video Coding (HEVC) (Heindel, A., et al 2016) was proposed. HEVC was employed for encoding the base layer. In addition, introduced a low-complexity method known as "Sample-based weighted prediction for Enhancement Layer Coding" (SELC) for compression of the enhancement layer. Furthermore, improvement layer compression with JPEG-LS and the scalable expansion of HEVC (SHVC) are evaluated. But, SELC approach performed very similar to JPEG-LS. An adaptive Synthetic Aperture Radar (SAR) image compression technique (Ji, X., & Zhang, G. 2016) was introduced. This algorithm performed three stages coding stage, decoding stage and training stage. In this approach, ensures the confidentiality of SAR image compression algorithm by the adaptive wavelet dictionary learning, obtains the large compression ratio with the sparse coefficient quantization coding, simultaneously, it was used to suppress the speckle noise on SAR image. However, perceptual confusion was obtained in SAR images.

3. Proposed Methodology

In this segment, we describe the GF scheme for image fusing which is used reduce memory size as well as to enhance the image quality after compressing the frames.

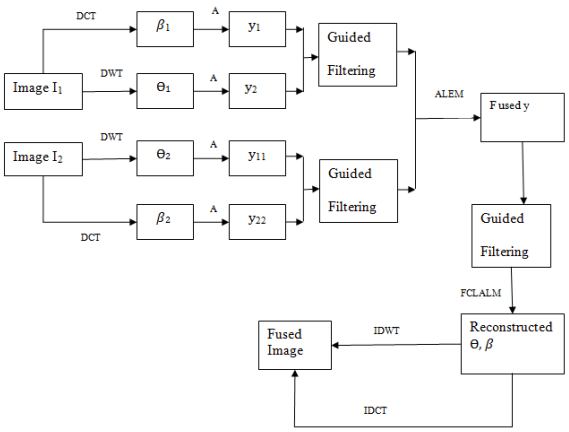

Figure 1: Guided Filtering Procedure

Guided Filtering

The guided filtering was calculated as follows:

$$a_k = (\Sigma_k + \epsilon U)\left(\frac{1}{|\omega|}\sum_{i\epsilon\omega_k} I_i p_i - \mu_k \bar{p}_k\right) \quad (1)$$

$$b_k = \bar{p}_k - a_k^T \mu_k \quad (2)$$

$$O_i = \bar{a}_i^T I_i + \bar{b}_i \quad (3)$$

where Σ_k denotes the 3×3 covariance matrix of I in ω_k, and U denotes the 3 × 3 identity matrix (Li et al 2013). The GF based on fusion technique and an AF was achieving the two-scale representations. Then, the detail and base layers are

fused via a GF based on weighted average technique.

Two-Scale Decomposition

The original videos or images are decomposed into two-scale demonstrations via AF. The base layer of every original image is achieved in below equation,

$$B_n = I_n * Z \quad (4)$$

In which, Z denotes the AF and B_n denotes the nth base layer, I_n denotes the nth original image and the amount of the AF are predictably locate to 31×31. As soon as the detail and base layer is achieved in below equation,

$$D_n = I_n - B_n \quad (5)$$

In which D_n represents the nth detail layer.

Weight Map Construction

This approach is constructed as follows. Laplacian filtering is applied to every original image to achieve the high-pass image H_n.

$$H_n = I_n * L \quad (6)$$

Where, H_n denotes the local average of the absolute value and to construct the saliency maps S_n and L denotes a 3 × 3 Laplacian filter.

$$S_n = |H_n| * g_{r_g,\sigma_g} \quad (7)$$

In which, the parameters r_g and σ_g are set to 5 and g denotes a Gaussian low-pass filter of range $(2r_g + 1)(2r_g + 1)$. The calculated saliency maps provide better description of the saliency level of complete information. The below equation of the saliency maps compared to establish the weight maps.

$$P_n^k = \begin{cases} 1 \; if \; S_n^k = \max(S_1^k, S_2^k, \ldots, S_N^k) \\ 0 \; otherwise \end{cases} \quad (8)$$

In which, S_n^k denotes the saliency rate of the pixel k in the nth video or image and N referred as number of original images. GF image is executed on every weight map P_n with the equivalent original image I_n portion as the guidance image.

$$W_n^B = G_{r_1,\epsilon_1}(P_n, I_n) \quad (9)$$

$$W_n^D = G_{r_2,\epsilon_2}(P_n, I_n) \quad (10)$$

In which, W_n^D and W_n^B denotes the weight maps of the detail and base layers and $r_1, \epsilon_1, r_2 \; and \; \epsilon_2$ denotes the parameters of the GF. The calculated values of the N weight maps are normalized such that they calculation to one at every pixel k.

Reconstruction Using Two-Scale

This scheme includes the below subsequent steps. Different original images in the detail and base layers be fused along with through weighted averaging

$$\bar{B} = \sum_{n=1}^{N} W_n^B B_n \quad (11)$$

$$\bar{D} = \sum_{n=1}^{N} W_n^D D_n \quad (12)$$

The fused image F is achieved through integrating the fused detail layer $\bar{D}$ and the fused base layer $\bar{B}$

$$F = \bar{B} + \bar{D} \quad (13)$$

4. Experimental Results

The comparison is prepared in terms of the overall presentation metrics called the Normalized Absolute Error Comparison, Maximum error rate, Mean Square Error (MSE), Maximum Difference Comparison and Peak Signal to Noise Ratio (PSNR) which is defined in the following sub segments. Finally the system propose an edge preserving image filtering method which is an adaptive local linear model and the principle of Stein's unbiased risk estimate (SURE) known as LLSURE.

Mean Square Error (MSE)

MSE among the decrypted and original images is computed. It is defined as:

$$MSE = \frac{1}{MN} \sum_{y=1}^{M} \sum_{x=1}^{N} [\, I(x,y) - I'(x,y)\,]^{2} \quad (14)$$

Where $I(x,y)$ refer as original image, $I'(x,y)$ indicates approximated version (which is actually the decompressed image), M and N denotes dimensions of the images. The graphical illustration of comparison of the proposed techniques with the existing techniques is given in the following figure 2.

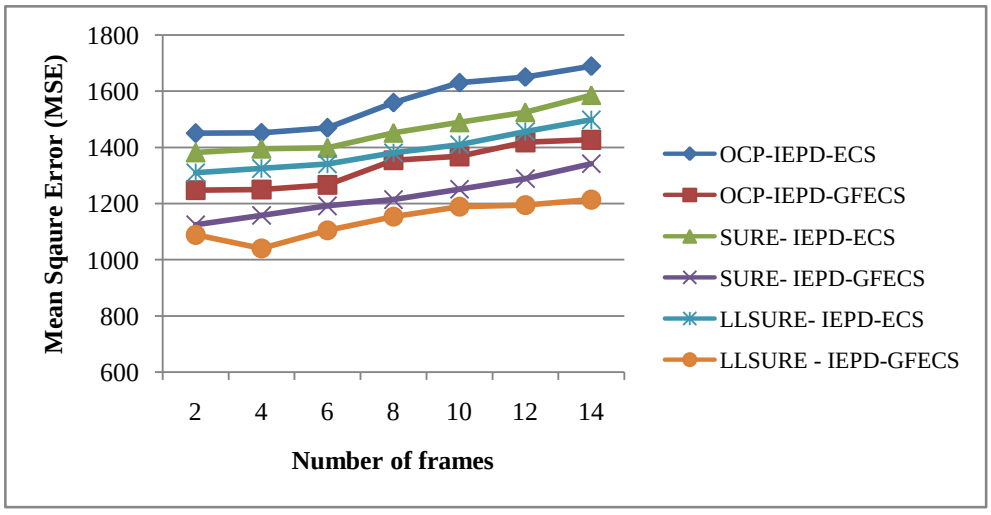

Figure 2: MSE Comparison vs. Comparison

Figure 2 shows that the comparison of OCP-IEPD-ECS, OCP-IEPD-GFECS, SURE- IEPD-ECS, SURE- IEPD-GFECS, LLSURE- IEPD-ECS and LLSURE - IEPD-GFECS techniques in terms of MSE. The X-axis the numbers of frames are taken. Y-axis mean square error values are taken. The MSE value decreased for proposed methods compare to existing method. The original measure values are indicated in the table 1.

Table 1: MSE Value vs. Comparison

No.of Frames	Mean Square Error(MSE)					
	OCP-IEPD-ECS	OCP-IEPD-GFECS	SURE-IEPD-ECS	SURE- IEPD-GFECS	LLSURE-IEPD-ECS	LLSURE - IEPD-GFECS
Frame 2	1450	1248	1382	1125	1310	1089
Frame 4	1452	1250	1395	1158	1325	1041
Frame 6	1469	1267	1398	1192	1341	1105
Frame 8	1559	1354	1452	1214	1381	1154
Frame 10	1630	1368	1489	1251	1410	1189
Frame 12	1650	1418	1525	1289	1456	1195
Frame 14	1689	1427	1586	1342	1498	1214

The MSE values of OCP-IEPD-ECS, OCP-IEPD-GFECS, SURE- IEPD-ECS, SURE- IEPD-GFECS, LLSURE- IEPD-ECS and LLSURE-IEPD-GFECS techniques are denoted in table format. The MSE value reduced for proposed OCP-IEPD-GFECS techniques compare to existing OCP-IEPD-ECS techniques.

Peak Signal to Noise Ratio (PSNR): To evaluate image compression quality by using the PSNR. This proportion is often used as a quality measurement among a compressed image and the original. PSNR represents a compute of the peak error. PSNR value of the proposed techniques must be excessive that represents the better compression quality of the videos without noise. The PSNR is approximate from the MSE

$$PSNR = 10\,log_{10}\left(\frac{R^2}{MSE}\right) \quad (15)$$

Where, MSE denotes Mean Square Error and R denotes Maximum fluctuation in the given image data type. The graphical illustration of the PSNR rate is given in the following figure 3 whose measurement values are obtained in the matlab simulation environment. In that graph, existing and the proposed techniques are compared with each other.

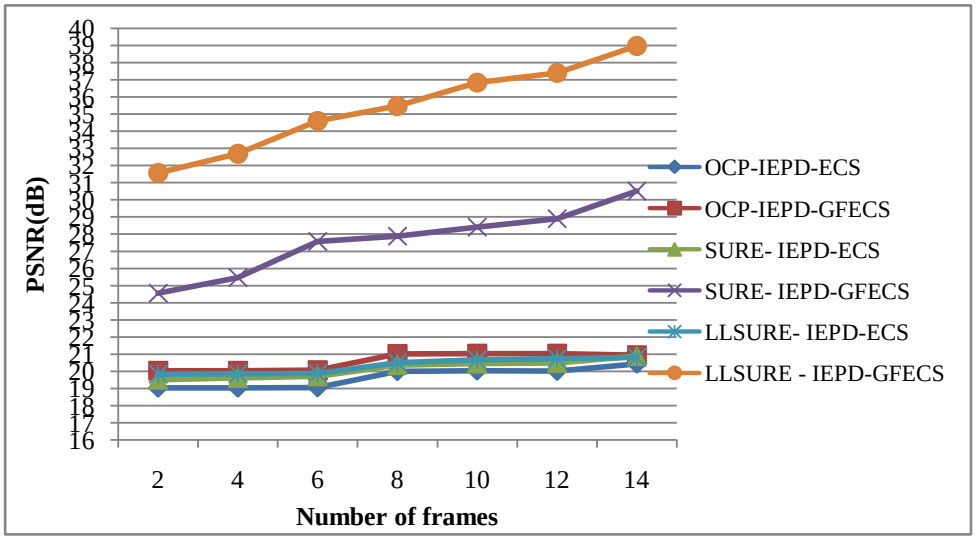

Figure 3: PSNR Comparison vs. Comparison

Figure 3 shows that the comparison of OCP-IEPD-ECS, OCP-IEPD-GFECS, SURE- IEPD-ECS, SURE- IEPD-GFECS, LLSURE- IEPD-ECS and LLSURE - IEPD-GFECS techniques in terms of PSNR value. The X-axis the numbers of frames are taken. Y-axis PSNR values are taken. The PSNR value increased for proposed methods compare to existing method. Mean square errors values in the graph show considerable improvement of the proposed methods. The original measure values are denoted in the table 2.

Table 2: PSNR Value vs. Comparison

No. of Frames	PSNR (dB)					
	OCP-IEPD-ECS	OCP-IEPD-GFECS	SURE-IEPD-ECS	SURE-IEPD-GFECS	LLSURE-IEPD-ECS	LLSURE - IEPD-GFECS
Frame 2	19.039	20.041	19.51	24.56	19.84	31.58
Frame 4	19.037	20.039	19.61	25.47	19.86	32.69
Frame 6	19.062	20.064	19.71	27.58	19.88	34.61
Frame 8	20	21.012	20.36	27.89	20.5	35.47
Frame 10	20.037	21.039	20.45	28.41	20.67	36.84
Frame 12	20.01	21.035	20.49	28.91	20.75	37.41
Frame 14	20.44	20.95	20.89	30.51	20.81	38.98

The PSNR values of OCP-IEPD-ECS, OCP-IEPD-GFECS, SURE- IEPD-ECS, SURE- IEPD-GFECS, LLSURE- IEPD-ECS and LLSURE - IEPD-GFECS techniques are represented in table format.

Maximum Error

It occurs at the margins of the bioequivalence interval and it increases as noise variance increases. It is directly proportional to the noise rate which will increases gradually for the increased value of the noise rate.

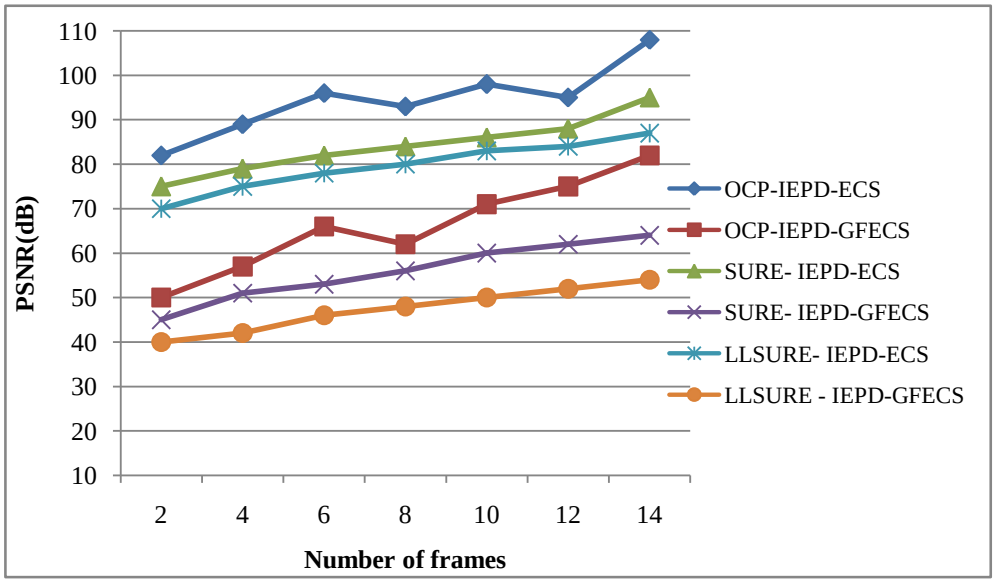

Figure 4: Maximum Error Comparison vs. Comparison

Figure 4 shows that the comparison of OCP-IEPD-ECS, OCP-IEPD-GFECS, SURE- IEPD-ECS, SURE- IEPD-GFECS, LLSURE- IEPD-ECS and LLSURE - IEPD-GFECS techniques in terms of Maximum Error value. The X-axis the

numbers of frames are taken. Y-axis Maximum Error values are taken. It is proves that the maximum error values of proposed methodology is lower than the existing approaches and the maximum error rate is increasing and decreasing in the proposed methodology in the non-linear sequence. The exact values of maximum error rate are given in the following Table 3.

Table 3: Maximum Error vs. comparison

No. of Frames	Maximum Error					
	OCP-IEPD-ECS	OCP-IEPD-GFECS	SURE- IEPD-ECS	SURE- IEPD-GFECS	LLSURE- IEPD-ECS	LLSURE - IEPD-GFECS
Frame 2	82	50	75	45	70	40
Frame 4	89	57	79	51	75	42
Frame 6	96	66	82	53	78	46
Frame 8	93	62	84	56	80	48
Frame 10	98	71	86	60	83	50
Frame 12	95	75	88	62	84	52
Frame 14	108	82	95	64	87	54

The maximum Error values of OCP-IEPD-ECS, OCP-IEPD-GFECS, SURE-IEPD-ECS, SURE- IEPD-GFECS, LLSURE- IEPD-ECS and LLSURE - IEPD-GFECS are represented in table format. The Maximum error values reduced for proposed methods compare to existing method.

Normalized Absolute Error Comparison (NAE)

Normalized absolute error comparison is used to predict the average of correct prediction that was made in terms of the predicted outcomes. Normalized absolute error is determining the average success rate of video compression which was made. The comparison of existing and proposed techniques in terms of normalized absolute error was given in the following Figure 5.

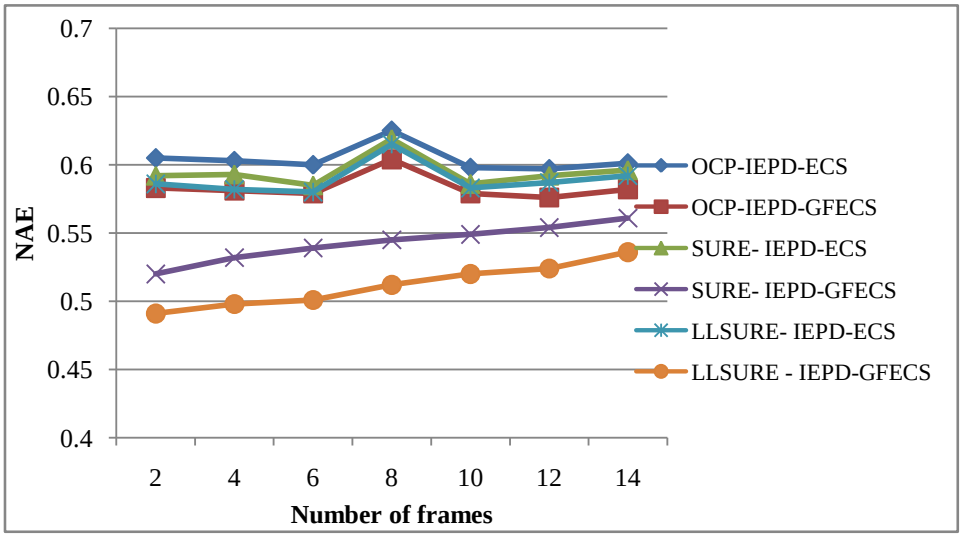

Figure 5: NAE Comparison

Figure 5 show that the comparison of OCP-IEPD-ECS, OCP-IEPD-GFECS, SURE- IEPD-ECS, SURE- IEPD-GFECS, LLSURE- IEPD-ECS and LLSURE - IEPD-GFECS techniques in terms of normalized absolute error values. The X-

axis the numbers of frames are taken. Y-axis normalized absolute error values are taken. The NAE values decreased for proposed method compare to existing method. The exact values of normalized absolute error rate are given in the following Table 4.

Table 4: Normalized Absolute Error Comparison

No. of Frames	Normalized Absolute Error(NAE)					
	OCP-IEPD-ECS	OCP-IEPD-GFECS	SURE- IEPD-ECS	SURE- IEPD-GFECS	LLSURE- IEPD-ECS	LLSURE - IEPD-GFECS
Frame 2	0.605	0.583	0.592	0.52	0.586	0.491
Frame 4	0.603	0.581	0.593	0.532	0.582	0.498
Frame 6	0.600	0.579	0.585	0.539	0.580	0.501
Frame 8	0.625	0.604	0.619	0.545	0.615	0.512
Frame 10	0.598	0.579	0.586	0.549	0.583	0.52
Frame 12	0.597	0.576	0.592	0.554	0.587	0.524
Frame 14	0.601	0.582	0.596	0.561	0.592	0.536

The Normalized Absolute Error values of OCP-IEPD-ECS, OCP-IEPD-GFECS, SURE- IEPD-ECS, SURE- IEPD-GFECS, LLSURE- IEPD-ECS and LLSURE-IEPD-GFECS system are represented in table format. The Normalized Absolute Error values of proposed technique are decreased compared to the existing method.

Maximum Difference Comparison

Maximum difference parameter is used to evaluate the variation present in the decompressed image than the compressed image in terms of improved performance ratio. The comparison of maximum difference parameter value is given in the following Figure 6.

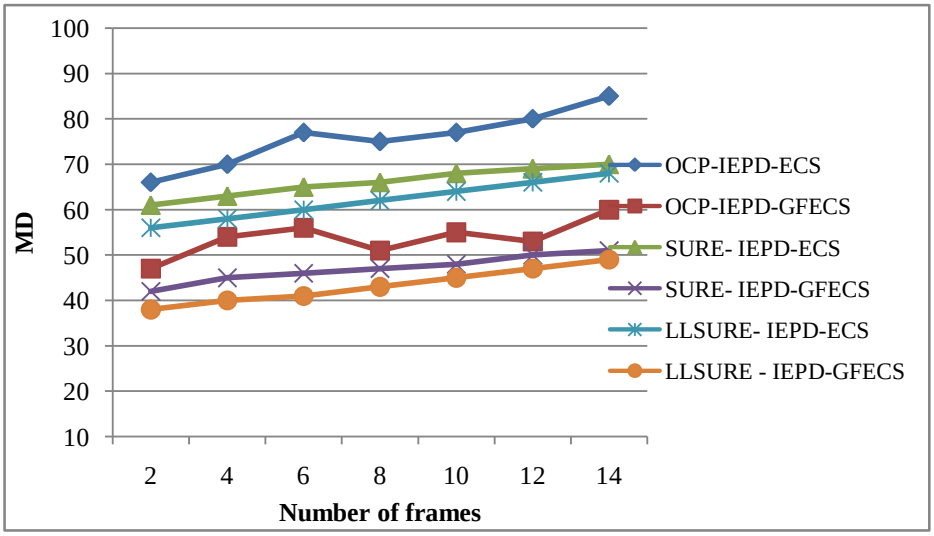

Figure 6: Maximum Difference Comparison

Figure 6 show that the comparison of OCP-IEPD-ECS, OCP-IEPD-GFECS, SURE- IEPD-ECS, SURE- IEPD-GFECS, LLSURE- IEPD-ECS and LLSURE - IEPD-GFECS techniques in terms of maximum difference values. The X-axis the numbers of frames are taken. Y-axis maximum difference values are taken. The maximum difference value decreased for proposed method compare to existing method. The exact values of maximum difference rate are given in the

following Table 5.

Table 5: Maximum Difference

No. of Frames	Maximum Difference					
	OCP-IEPD-ECS	OCP-IEPD-GFECS	SURE- IEPD-ECS	SURE- IEPD-GFECS	LLSURE- IEPD-ECS	LLSURE - IEPD-GFECS
Frame 2	66	47	61	42	56	38
Frame 4	70	54	63	45	58	40
Frame 6	77	56	65	46	60	41
Frame 8	75	51	66	47	62	43
Frame 10	77	55	68	48	64	45
Frame 12	80	53	69	50	66	47
Frame 14	85	60	70	51	68	49

The Maximum Difference values of OCP-IEPD-ECS, OCP-IEPD-GFECS, SURE- IEPD-ECS, SURE- IEPD-GFECS, LLSURE- IEPD-ECS and LLSURE - IEPD-GFECS are represented in table format. The Maximum Difference values of proposed technique are reduced compared to the existing technique.

5. Conclusion and Future Work

In this paper, we propose the guided filtering (GF) scheme for image fusing (IF). This technique is used to decrease memory size as well as to enhance the image quality after compressing the frames. The IF is used for incorporating related information from more images into a single image. The ensuring image may be more informative than any other input images. Guided filter has less computation time which is independent of filtering size. In this approach, first the image will be changed into the two scale representation via applying the AF (average filtering) methods. This scheme enhances the image quality after compressing the frames. Experimental outcomes show that our proposed scheme is providing better results in terms of Maximum error comparison, Peak Signal to Noise Ratio (PSNR), Normalized Absolute Error (NAE), Maximum Difference (MD) and Mean Square Error(MSE). Application of HDCT-DWT compression is also extended to the field of mobile communications. The simplicity and regularity of the method makes it suitable to be implemented on programmable logic devices, such as Field Programmable Gate Arrays (FPGA's) in custom Very-large-scale integration (VLSI) integrated circuits.

References

[1] He K., Sun J., Tang X., Guided image filtering, IEEE transactions on pattern analysis and machine intelligence 35(6) (2013), 1397-1409.

[2] Li Z., Zheng J., Zhu Z., Yao W., Wu S., Rahardja S., Content adaptive bilateral filtering, IEEE International Conference on Multimedia and Expo Workshops (2013), 1-6.

[3] Phan C., Ha S., Jeon J., Adaptive guided image filtering for sharpness enhancement and noise removal, Advances in image and video technology, Springer Berlin Heidelberg (2012).

[4] Shi S., Gioia P., Madec G., Efficient compression method for integral images using multi-view video coding, 18th IEEE International Conference on Image Processing (2011), 137-140.

[5] Zuo Z., Lan X., Deng L., Yao S., Wang X., An improved medical image compression technique with lossless region of interest, Optik-International Journal for Light and Electron Optics 126(21) (2015), 2825-2831.

[6] Li S.A., Tsai C.Y., Low-cost and high-speed hardware implementation of contrast-preserving image dynamic range compression for full-HD video enhancement, IET Image Processing 9(8) (2015), 605-614.

[7] Kamisli F., Block-based spatial prediction and transforms based on 2D Markov processes for image and video compression, IEEE Transactions on Image Processing 24(4) (2015), 1247-1260.

[8] Zhou N., Pan S., Cheng S., Zhou Z., Image compression–encryption scheme based on hyper-chaotic system and 2D compressive sensing, Optics & Laser Technology 82 (2016), 121-133.

[9] Kekre H.B., Natu P., Sarode T., Color image compression using vector quantization and hybrid wavelet transform, Procedia Computer Science 89 (2016), 778-784.

[10] Heindel A., Wige E., Kaup A., Low-Complexity Enhancement Layer Compression for Scalable Lossless Video Coding based on HEVC, IEEE Transactions on Circuits and Systems for Video Technology (2016).

[11] Ji X., Zhang G., An adaptive SAR image compression method, Computers & Electrical Engineering (2016).

[12] Li S., Kang X., Hu J., Image fusion with guided filtering, IEEE Transactions on Image Processing 22(7) (2013), 2864-2875.